Research article

Journal of Human, Health and Halal Metrics; 2024, 5(2): 66-79
https://doi.org/10.30502/jhhhm.2025.504496.1103

Fabrication and characterization of chitosan/polyethylene oxide/*Arctium lappa* L. extract/graphene oxide nanofibrous scaffold for wound healing purposes

Hossein Motahhary[1], Arash Montazeri[1*], Rasoul Shemshadi[2], Hossein Rastegar[3], Dehghan Navaei Ardeh[4]

1- Department of Nanotechnology, Faculty of Engineering, University of Guilan, Rasht, Iran.
2- Department of Chemical Industry, National University of Skills (NUS), Tehran, Iran.
3- Halal Research Center of IRI., Food and Drug Administration, Ministry of Health and Medical Education, Tehran, Iran.
4- Biomedical Engineering Biomaterials, Faculty of Materials and Metallurgical Engineering, Semnan University, Semnan.

Submission: 5 November 2024 ***Revision***: 25 November 2024 ***Acceptance***: 10 December 2024

Abstract

Background and Objective: Due to the cell affinity of chitosan (CS), the hydrophilicity of polyethylene oxide (PEO), and the antibacterial activity of plant-derived compounds such as *Arctium lappa* L. (*A. lappa*) extract, a CS/PEO/*A. lappa* nanofiber reinforced with graphene oxide (GO) can be extensively used as wound healing dressings for skin tissue regeneration. Therefore, in this study, CS/PEO nanofibrous scaffolds containing different concentrations of extract and GO were fabricated using the electrospinning method.

Materials and Methods: The CS/PEO scaffolds with a weight ratio of 1:2, containing different concentrations of *A. lappa* extract (15, 25, and 35% w/w), were fabricated using the electrospinning method. The optimal concentration of extract was 25% w/w based on the nanofibers' average diameter and its lower standard deviation. Then, 0.5 and 1% w/w of GO was added to the optimal solution of CS/PEO/*A. lappa* extract. The scaffolds were characterized by X-ray diffraction (XRD), field emission scanning electron microscopy (FE-SEM), energy dispersive X-ray analysis (EDX), thermogravimetric analysis (TGA), and antibacterial evaluation.

Results and Conclusion: FE-SEM studies revealed that smooth, uniform, and defect-free electrospun nanofiber scaffolds were obtained between the average diameter of 226.61 ±14 and 643 ±152 nm. By addition of GO 1% w/w to CS/PEO/*A. lappa* 25% w/w, gram-negative bacteria (*Escherichia coli* and *Pseudomonas aeruginosa*) were better inhibited than gram-positive bacteria (*Staphylococcus aureus*). We concluded that incorporation of *A. lappa* extract and GO into CS/PEO nanofiber scaffold could improve its antibacterial and structural properties, making it suitable for potential biomedical applications.

Keywords: Antibacterial activity, *Arctium lappa* L. extract, Chitosan-polyethylene oxide nanofiber, Electrospinning, Graphen oxide

1. Introduction

Skin is the largest organ of the body, composed of epidermis, dermis, and hypodermis layers tasked with protecting internal organs, controlling body temperature, and producing vitamin D. Moreover, these layers efficiently support the body's balance and stability [1,2]. External or internal factors can lead to the disruption of skin integrity, resulting in wounds [3]. Cell coordination is crucial in skin repair process, encompassing hemostasis, inflammation, tissue proliferation, and regeneration stages [4-7]. Properly dressing a wound is essential for effective healing. The limitations of existing dressings in adapting to changing wound conditions and their

* Correspondence to: Arash Montazeri; E-mail: A.montazeri@guilan.ac.ir; Tel.: +98-1333690274; Fax: +98-1333690270

unsuitability for specific body parts have fueled the growing demand for innovative smart dressings [8]. Traditional wound dressings are cost-effective but have limited functionality and may adhere to the wound, causing pain. Innovative wound dressings, combining modern technologies like hydrogels, nanoparticles, and electrospun nanofibers accelerate wound healing. Electrospinning technology, in particular, has garnered significant attention in this field [9].

Nanofibers are highly beneficial for wound healing due to their high porosity, large surface area, and interconnected pores, which support cell growth, blood vessel formation, and nutrient transfer while preventing bacterial entry. Their versatility in using biocompatible polymers from natural or synthetic sources and the flexibility of the electrospinning process to incorporate therapeutic agents make them ideal for wound care applications. Additionally, electrospinning is a simple and efficient method for producing these ultrafine fibers, making it a preferred technique for fabricating one-dimensional nanostructured materials [10,11].

Chitosan (CS), due to its antimicrobial, antioxidant, and anti-inflammatory properties is used as a therapeutic polymer. This biocompatible and biodegradable polymer can be combined with other chemicals and used in the form of films, beads, powders, capsules, and nanofibers. Electrospinning of pure CS solution is challenging due to its high viscosity and practical inconveniences. Therefore, combining it with other polymers like polyethylene oxide (PEO) can improve this process [12-14]. PEO enhances thermal stability and porosity when combined with CS and other polymers due to its biocompatibility, mechanical strength, low toxicity, and spinnability [15,16].

Burdock species, particularly *Arctium lappa* L., is a perennial plant from the *Compositae* family, 1 to 1.5 m tall, with broad leaves and spindle-shaped roots. It is found in many countries in the Middle East, Asia, and Europe, and is used as an anti-inflammatory, antimicrobial, antidiabetic, antiviral, blood purifier, and hepatoprotective drug [17]. The main active ingredients isolated from this plant are tannin, arctigenin, arctin, beta-odesmol, caffeic acid, chlorogenic acid, inulin, trichogenin-4, sitosterol-beta-D-glucose, pranoside, lapaul F, diarctigenin, and beta-desmol. Apart from these compounds, burdock also contains nutrients, including various vitamins such as C, B_1, B_2, B_3, B_6, B_{12}, E, and amino acids [18]. *A. lappa* L. is widely used in traditional medicine for treating skin disorders, diabetes, and blood detoxification. Its extracts help strengthen the immune system and enhance metabolic functions [18,19]. The root of the plant contains compounds that can inhibit the growth of cancer cells and induce their programmed cell death (apoptosis). However, consuming some of these compounds in high doses may lead to side effects [18,20].

Graphene oxide (GO), a carbon sheet with oxygen groups derived from the oxidation of graphite, stands out due to its low production cost, water solubility, and antimicrobial properties. These characteristics make it a promising material for drug delivery and disinfection. However, its potential toxicity at high concentrations warrants careful consideration [21,22].

Based on these properties, this study explores the fabrication and characterization of novel electrospun nanofibrous scaffolds composed of CS, PEO, *A. lappa* extract, and GO. According to our research, this is the first investigation of such a combination of materials in electrospun nanofibers. By varying the concentrations of GO, we aimed to optimize the properties of these scaffolds for potential wound dressing applications.

2. Materials and Methods

2.1. Materials

CS with medium molecular weight and PEO with a molecular weight of 1000 kDa were purchased from Sigma-Aldrich (USA). Acetic acid, dimethyl sulfoxide (DMSO), Mueller-Hinton agar (MHA), and Triton X-100 were prepared from Merck (Germany), and ethanol was purchased from

Gostaran Pars Nanomaterials Company (Iran). GO nano-colloid containing single-layer GO sheets with a sheet size of 3-7 μm, sheet thickness of 0.8-1.2 nm, at concentration of 4 g/l was manufactured by Nanomavad Gostaran Pars Company (Iran). *A. lappa* plant was purchased from Barijessence Pharmaceutical co. (Kashan, Iran). For anti-bacterial tests, three bacterial strains of *Escherichia coli* (ATCC 35218), *Staphylococcus aureus* (ATCC 25923), and *Pseudomonas aeruginosa* (ATCC 27853) were used. Bacterial strains were provided by the Department of Food Science, Technology, and Engineering of Guilan University.

2.2. Extraction of *A. lappa* extract

Maceration method was used to extract the bioactive compounds from *A. lappa*. Fresh leaves were washed with distilled water in three stages and sun-dried further for 48 h. Then, the dried leaves were pulverized into a fine powder using an electric grinder. The powdered plant was mixed with ethanol 70% in 1:20 ratio, and subjected to constant agitation at room temperature for 72 h. The final mixture was filtered to remove solid residue, and the filterate was concentrated using an oven at 50 °C to evaporate the solvent. The semi-solid concentrated extract was stored at 4 °C for further analysis [23,24].

2.3. Preparation of CS/PEO nano-fibers

CS/PEO solution was prepared by dissolving 0.6 g of CS and 0.3 g of PEO powder at 2:1 mass ratio in acetic acid 45%. Then, Triton X-100 1% as emulsifier and DMSO 10% as co-solvent were added to the mixture [25]. The solution was stirred for 24 h at room temperature using a magnetic stirrer. In the next step, the polymer solution was added to a 5 ml syringe with a fine needle (0.9 mm in diameter). Finally, the polymer solution was placed in the infusion pump of the electrospinning device, and aluminum foil was utilized on the collector to gather the formed fibers. The electrospinning parameters, such as voltage and the distance between the needle tip and the collector were adjusted, while the polymer solution's weight ratio was kept constant. The details are presented in Table 1. Scanning Electron Microscope (SEM) imaging was done on the CS/PEO nanofibers to determine the optimum nanofiber scaffold. To ensure the production of high-quality nanofibers, the polymer solution flow rate in the electrospinning process was set on 0.4 ml/h, which was consistent with the optimal flow rate reported in previous study [26].

Table 1- Electrospun parameters for fabrication of nanofibrous scaffolds

Sample	Voltage (kv)	Nozzle-to-collector distance (cm)	Flow rate (ml/h)
A_1	16	18	0.4
A_2	18	18	0.4
A_3	20	18	0.4
A_4	20	16	0.4
A_5	20	14	0.4

2.4. Preparation of CS/PEO/*A. lappa* extract scaffolds

A. lappa extract was added to the CS/PEO optimum solution at concentrations of 15, 25, and 35% w/w. The solutions were stirred for 12 h by a magnetic stirrer. The final solutions were then electrospun under the optimized condition determined for CS/PEO nanofiber scaffold in the last step. After electrospinning, SEM analysis was conducted to evaluate the structure of nanofibers.

2.5. Preparation of CS/PEO/*A. lappa* extract/GO nanocomposites

To improve the properties of nanofibers, different amounts of GO (0.5 and 1% w/w) were added to the basic polymer solution of CS/PEO and CS/PEO/*A. lappa* extract. First, GO was added to distilled water and subjected to ultrasonication for 15 min with power of 120 W to achieve complete dispersion. Then, CS/PEO and the extract were added, and the mixture was stirred for 12 h to obtain a homogeneous

mixture. Finally, the mixture was subjected to ultrasonication for additional 10 min to ensure the dispersion of GO.

2.6. Characterization

2.6.1. X-ray diffraction (XRD)

For this study, an X-ray diffractometer (Philips model PW1730, Netherlands) was employed. X-ray diffraction patterns were collected at voltage of 23 kV and current of 33 mA, using Cu Kα radiation with a wavelength (λ) of 1.52356 Å, and a scan rate of 3.35 degrees per second over a 2θ range of 5 to 60 degrees.

2.6.2. SEM

For evaluation of morphology and average diameter of the nanofibers, as well as the interconnectivity of the nanofiber pores and cell adhesion, an SEM (Philips model XL30S, Netherlands) operating at 20-25 kV was used.

2.6.3. Energy-dispersive X-ray spectroscopy (EDX)

EDX analysis was performed using a TESCAN MIRA3 field emission scanning electron microscope (FE-SEM) from the Czech Republic, with an accelerating voltage of 10 kV. The samples were meticulously prepared and analyzed under controlled environmental conditions.

2.6.4. Thermogravimetric analysis (TGA)

To analyze the thermal properties of both pure materials and nanofibers, a Thermo Scientific NIKOLET thermal balance was used. The experiments were carried out under an argon atmosphere within a temperature range of 40 to 600 °C, with a heating rate of 10 °C/min.

2.6.5. Antibacterial activity of nanofibers

The antibacterial activity of the scaffolds was evaluated by disk diffusion method on two species of gram-negative bacteria (*E. coli* and *P. aeruginosa*) and one species of gram-positive bacteria (*S. aureus*). Microbial culture medium was prepared according to the manufacturer's protocol and poured into 10 cm plates. Then, a 0.5 McFarland bacterial suspension was prepared, and was cultured on the surface of Mueller-Hinton agar by sterilized cotton swabs. In the next step, the scaffolds were punched into circles with a diameter of 6 mm, and placed on the innoculated plates, followed by incubation at 37 °C for 24 h. Finally, the inhibition zones around the scaffolds were measured.

2.7. Statistical analysis

The data were examined using the statistical software Image J Version 1.52v and Origin Prolab version 9.9.

3. Results and Discussion

3.1. Characterization of nanofibrous scaffolds

3.1.1. Morphology

The CS/PEO scaffolds were fabricated by changing the parameters of the electrospinning method (Table 1), and morphology of the CS/PEO scaffolds is shown in Figure 1. SEM images revealed that the morphology of the CS/PEO scaffolds was significantly influenced by varying electrospinning parameters.

As indicated, the samples A_1, A_2, and A_4 resulted in nanofibers with higher adhesion and low porosity. In the sample A_5, electrospinning became difficult, and the nanofibrous structure was not formed. Based on these findings, the optimal condition was achieved by flow rate of 0.4 ml/h, a nozzle-to-collector distance of 18 cm, and a voltage of 20 kV (sample A_3), yielding scaffolds with interconnected pores and a uniform, defect-free nanostructure.

After determining the optimal electrospinning parameters for the CS/PEO scaffold, nanofibers with 15, 25, and 35% w/w extract were fabricated (Figures 2 b-d). The average diameter of the CS/PEO nanofibers was 226.61 ±14 nm. After addition of the extract, the diameter increased to 643.57 ±152 nm at 35% w/w loading, while maintaining a bead-free morphology. This increase in diameter was due to the higher viscosity of the polymer solution caused by the extract [27-29]. Based on the nanofibers' average diameter and its lower standard deviation, the scaffolds with 25% w/w *A. lappa* were selected as the optimum sample [30,31].

Study of Mir et al. showed that changing the mass ratio of CS/PEO significantly affects the fibers' diameter. Increasing the concentration of CS results in thinner fibers, while decreasing the concentration of PEO increases the electrical conductivity and viscosity of the solution, leading to a reduction in the fibers' diameter. A ratio of 2:1 CS/PEO was optimal for producing nanofibers with smaller diameters [17].

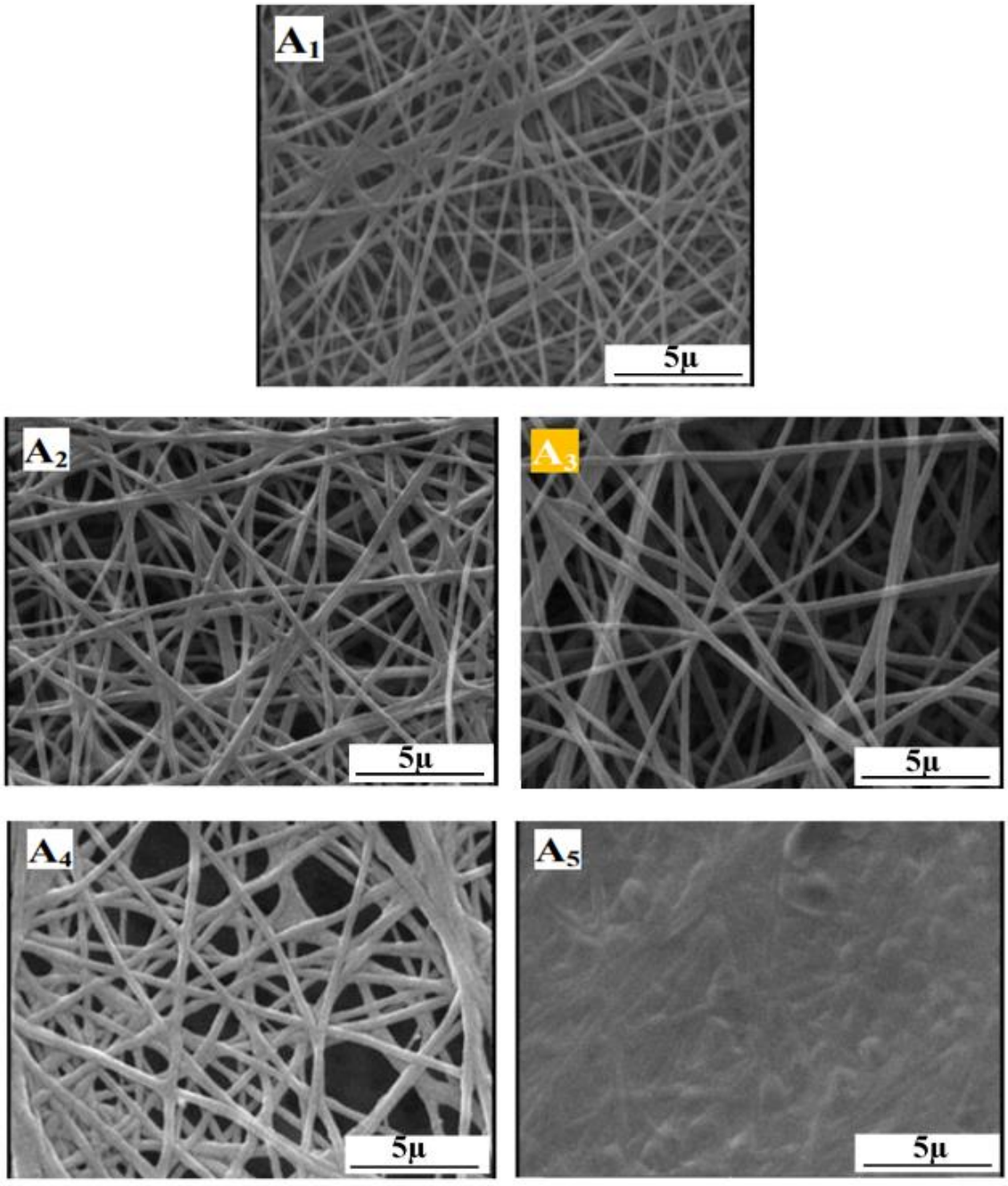

Figure 1- SEM images of CS/PEO (2:1) electrospun scaffolds with flow rate of 0.4 ml/h; A_1: V=16 KV, D=18 cm; A_2: V=18 KV, D=18 cm; A_3: V=20 KV, D=18 cm; A_4: V=20 KV, D=16 cm; A_5: V=20 KV, D=14 cm

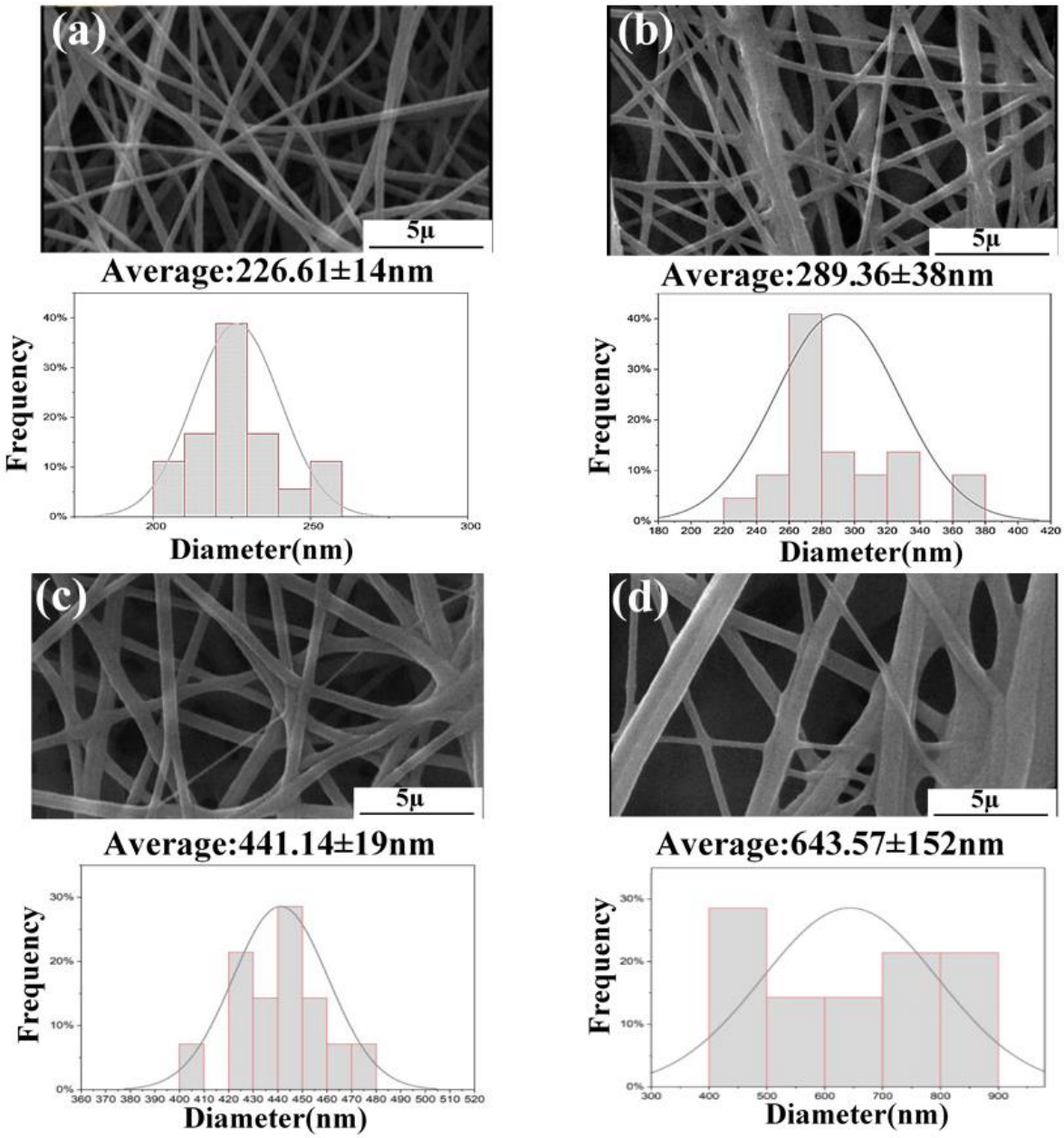

Figure 2- FE-SEM images of a) CS/PEO nanofibers (A_3), b) nanofiber scaffolds containing 15% w/w extract, c) nanofiber scaffolds containing 25% w/w extract, d) nanofiber scaffolds containing 35% w/w extract

After determining the optimal percentage of the extract to improve the nanofibers properties, different percents of GO were incorporated into the CS/PEO blends. Figures 3 a and b show that average diameter of the nanofibers increases by increasing the concentration of GO. This increase in nanofiber diameter was attributed to the increased viscosity and faster evaporation of the solvents (water, acetic acid, and DMSO) at higher concentrations [32]. In the next step, CS/PEO/25% w/w extract nanofibers containing 0.5 and 1% w/w GO were fabricated with the optimum electrospinning parameters. The FE-SEM images and the nanofibrous average diameter are shown in Figures 3 c and d.

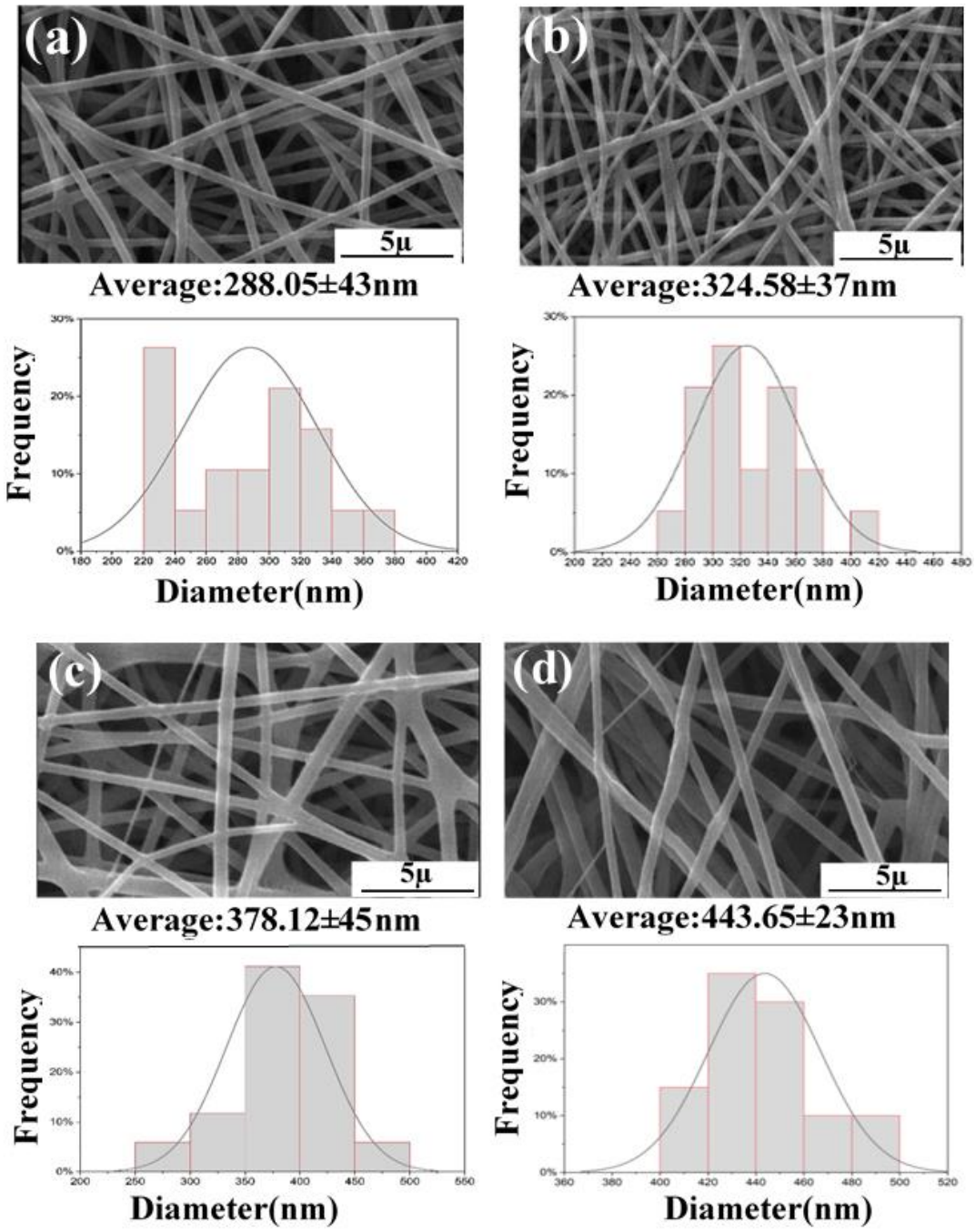

Figure 3- FE-SEM images of a) CS/PEO nanofiber containing 0.5% w/w GO, b) CS/PEO nanofiber containing 1% w/w GO, c) CS/PEO nanofiber containing 25% w/w extract and 0.5% w/w GO, d) CS/PEO nanofiber containing 25% w/w extract and 1% w/w GO

Mahdizadeh et al. demonstrated that incorporating GO into a CS polymer matrix increases the nanofiber diameter. The diameter distribution analysis revealed a progressive increase in mean nanofiber diameter with increasing GO concentration. Specifically, the mean diameters were 105.11, 121.37, and 159.59 nm for CS, CS/0.5% w/w GO, and CS/1% w/w GO, respectively. These findings suggest the formation of crosslinks between the polymer chains facilitated by the incorporation of GO [33].

Cailiao et al. indicated that low GO content (0.5% w/w) enhanced PEO chain alignment in GO/PEO nanofibers via hydrogen bonding between GO and PEO during electrospinning. Conversely, higher GO content increases solution viscosity, impeding PEO alignment [34].

3.1.2. XRD

The XRD pattern of CS, PEO, CS/PEO, *A. lappa* extract, and CS/PEO/25% w/w extract/1% w/w GO scaffold is presented in Figure 4. The characteristic peaks of the extract were formed at 2θ = 20.3°, corresponding to the Miller indices of the reflective planes (200) [35]. For pure CS, a broad peak at 2θ = 20° was observed, corresponding to its crystalline index [36], while pure PEO showed peaks at 19° and 23.3°, indicating its highly crystalline structure indexed to (120) and concerted (112) planes, respectively, according to the standard XRD data (PCPDF File nos. 49-2200 and 49-2201) [37]. After addition of PEO to CS, the reflection of both PEO peaks declined to a flat pattern. The CS/PEO nanofiber scaffold showed two distinct peaks at approximately 19.65° and 24°. The intensity of these peaks was significantly lower than that of pure PEO, indicating the influence of CS on the overall structure of the scaffold. Studies have shown that combining PEO with CS matrix improves the overall properties of the scaffold. This improvement may be due to intermolecular interactions between two polymers (formation of hydrogen bonds between CS and PEO), which contribute to changes in the crystalline structure of the components and prevent the appearance of sharp, high-intensity peaks [36,38,39]. As shown in Figure 4, the peak intensity of the CS/PEO nanofibers containing 25% w/w extract was less than that of CS/PEO nanofibers. The decrease in the intensity of the main diffraction line indicates a reduction in the degree of CS/PEO crystallinity. Moreover, in the nanofibers containing 25% w/w extract, the characteristic crystalline peaks of CS/PEO nanofibers shifted to 2θ = 18.97° and 22.19°. It appears that phenolic compounds present in the extract, such as plant hormones and polyphenolic acid, can penetrate into the space between polymer chains, enhancing intermolecular interaction and reducing the distance between chains [40].

XRD pattern of CS/PEO/25% w/w extract/1% w/w GO nanocomposite was similar to that of CS/PEO polymer containing the extract. As indicated, GO was uniformly dispersed in CS/PEO blend and the XRD peaks were a bit sharper than those achieved for CS/PEO/extract.

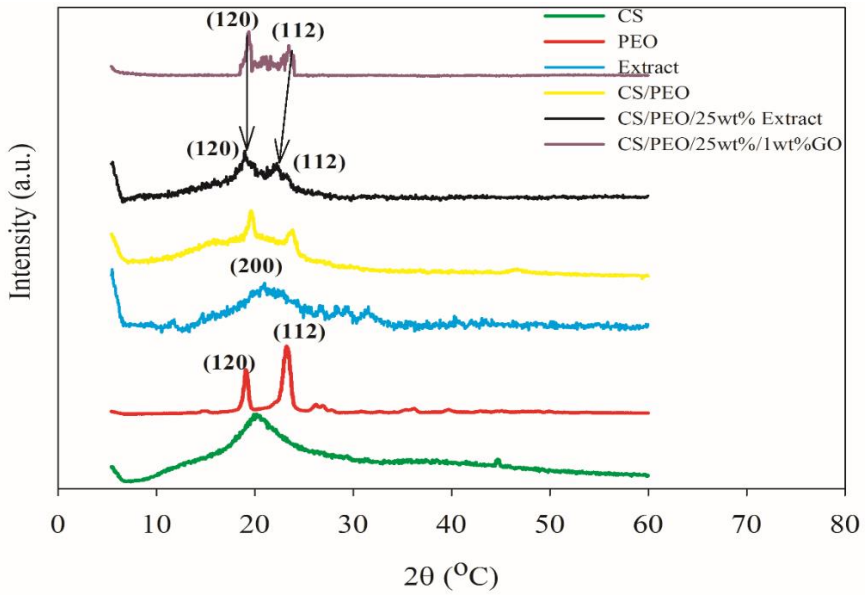

Figure 4- XRD spectra of CS, PEO, CS/PEO nanofiber, *A. lappa* extract, CS/PEO/25% w/w extract nanofiber, and CS/PEO/25% w/w extract/1% w/w GO nanofiber

3.1.3. EDX

Figure 5 illustrates EDX analyses of CS/PEO/25% w/w extract/1% w/w GO nanocomposite, which represents the quantitative analysis used to confirm the extract's presence and GO in the nanofiber scaffold. The carbon (C) and oxygen (O) peaks are the main elements, while N, Na, Mg, Cl, K, Ca, Mn, Fe, and Zn are related to the mineral elements in the extract mixed with CS/PEO/GO [41].

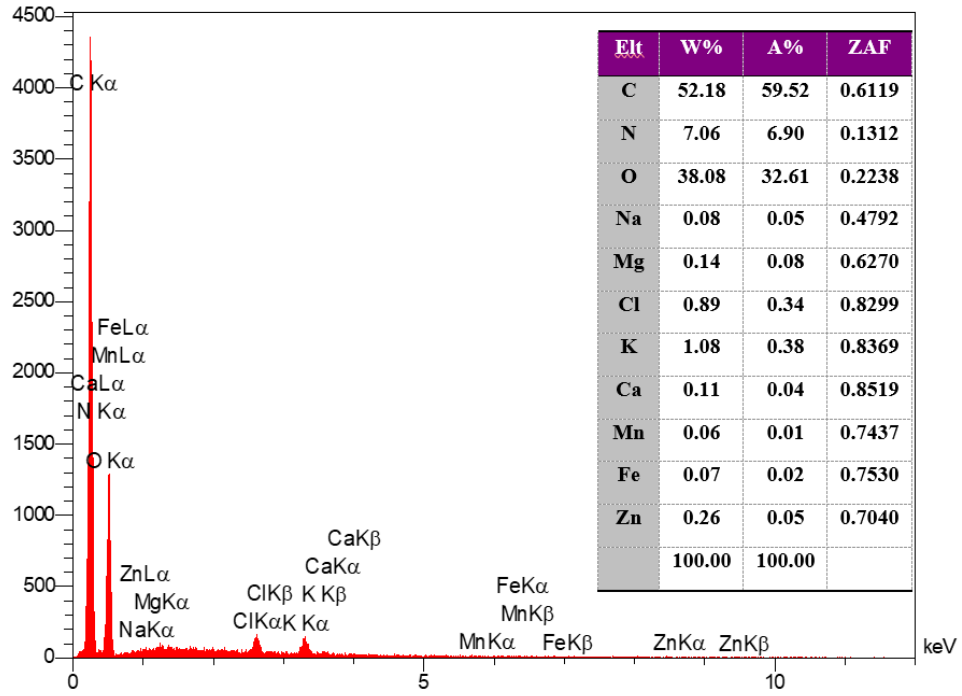

Elt	W%	A%	ZAF
C	52.18	59.52	0.6119
N	7.06	6.90	0.1312
O	38.08	32.61	0.2238
Na	0.08	0.05	0.4792
Mg	0.14	0.08	0.6270
Cl	0.89	0.34	0.8299
K	1.08	0.38	0.8369
Ca	0.11	0.04	0.8519
Mn	0.06	0.01	0.7437
Fe	0.07	0.02	0.7530
Zn	0.26	0.05	0.7040
	100.00	100.00	

Figure 5- EDX spectra analyses of CS/PEO/25% w/w extract/1% w/w GO nanofiber scaffold

3.2. TGA

TGA curves of CS/PEO, CS/PEO/25% w/w extract, and nanocomposites containing 0.5 and 1% w/w GO are shown in Figure 6. The CS/PEO nanofibers exhibit a three-step weight loss. The initial stage involved a 4% weight loss between 40-95 °C due to water evaporation. The second weight reduction (34%) resulted from thermal decomposition of CS chains. The third stage, with a 47% mass loss, was attributed to thermal decomposition of PEO component. A significant weight loss of 81% was observed between 237 and 440 °C, attributed to the breakdown of inter- and intra-linkages within PEO and CS chains. According to Figure 6, addition of 25% w/w extract to CS/PEO polymer did not alter the decomposition onset temperature. However, the residual char value of CS/PEO/25% w/w extract composite was affected. The residual char values of CS/PEO and CS/PEO/25% w/w extract at 550 °C were 13 and 25%, respectively. It seems that the presence of the extract postponed the decomposition of CS/PEO nanofiber.

Moreover, CS/PEO/25% w/w extract/0.5% w/w GO nanocomposite exhibited better thermal stability than CS/PEO and CS/PEO/25% w/w extract scaffolds. The degradation stages shifted toward higher temperatures when GO was added to CS/PEO scaffold, and the major decomposition initiation temperature (T_i) for CS/PEO/25% w/w extract and CS/PEO/25% w/w extract/0.5% w/w GO nanocomposite was about 246 and 264 °C, respectively. The thermal stability of the nanocomposites was enhanced due to hydrophilic and electrostatic interactions between CS and GO [42]. Proper dispersion of GO sheets in the polymer matrix also plays an essential role. These factors prevent the slip of polymer chains during heat treatment in the

weight loss test. For CS/PEO/25% w/w extract/1% w/w GO, T_i decreased to 247 °C. It is assumed that the presence of agglomerates due to the high weight percentage of GO decreased the thermal stability of the nanocomposite.

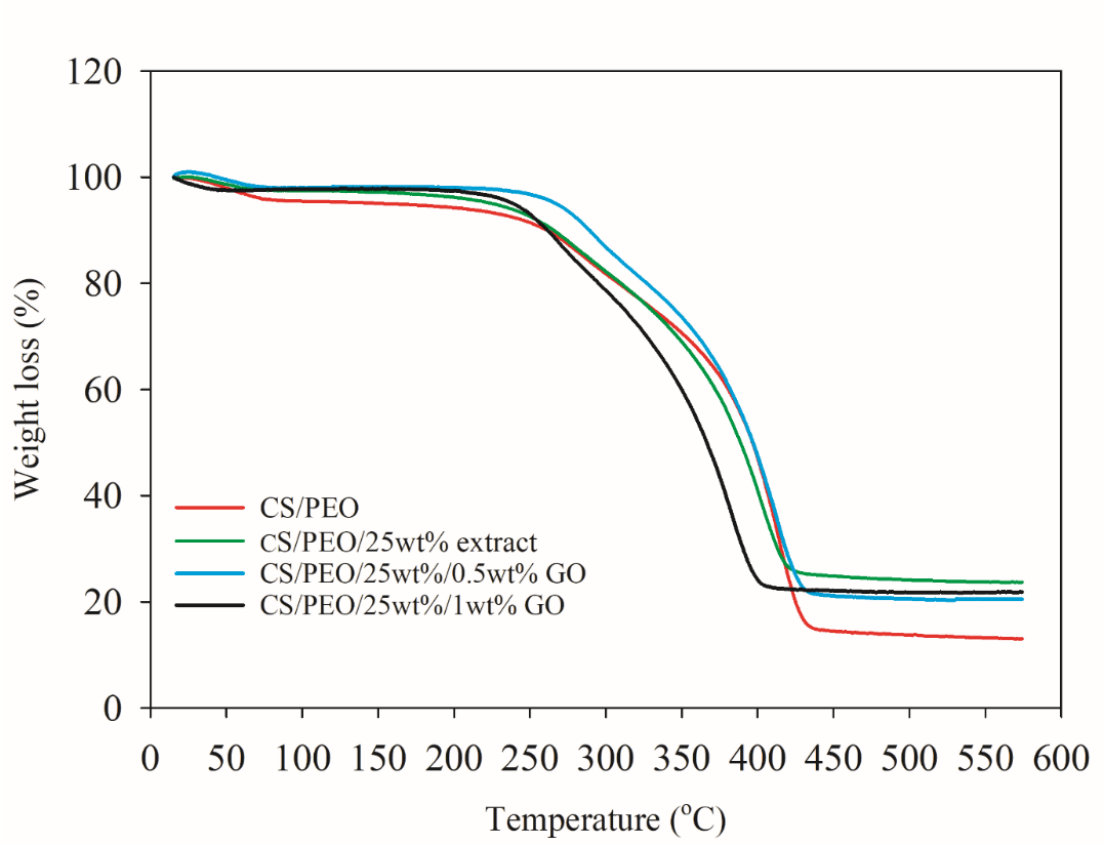

Figure 6- TGA curves of CS/PEO nanofibrous scaffolds at heating rate of 5°C/min

3.3. Antibacterial assessment of nanofiber scaffolds

Agar disk diffusion assay was used to evaluate the antibacterial activity of CS/PEO nanofibrous scaffolds and CS/PEO scaffolds containing 25% w/w extract with 0.5 and 1% w/w GO. Most reported studies have used only two bacterial strains, *S. aureus* and *E. coli*, providing a limited view of the antibacterial effects. This study also included *P. aeruginosa*, a multidrug-resistant Gram-negative bacterium associated with severe nosocomial infections. As shown in Figure 7, the inhibition zone of CS/PEO nanofibers against *S. aureus* was 8.5 mm, while those for *E. coli* and *P. aeruginosa* were 10 mm. In contrast, these values were 15, 19, and 18 mm for CS/PEO/25% w/w extract/1% w/w GO scaffolds, respectively. The results showed that the highest antibacterial activity among CS/PEO scaffolds was associated with CS/PEO/25% w/w extract nanofibers containing 1% w/w GO. Increased amount of GO resulted in a larger inhibition zone due to the highest level of oxidative stress and excessive production of reactive oxygen species by GO as well as physical damage to the cell membrane through its direct contact with the sharp edges of GO nanosheets. This finding emphasizes the potential of nanofibrous scaffolds to enhance antibacterial properties [22].

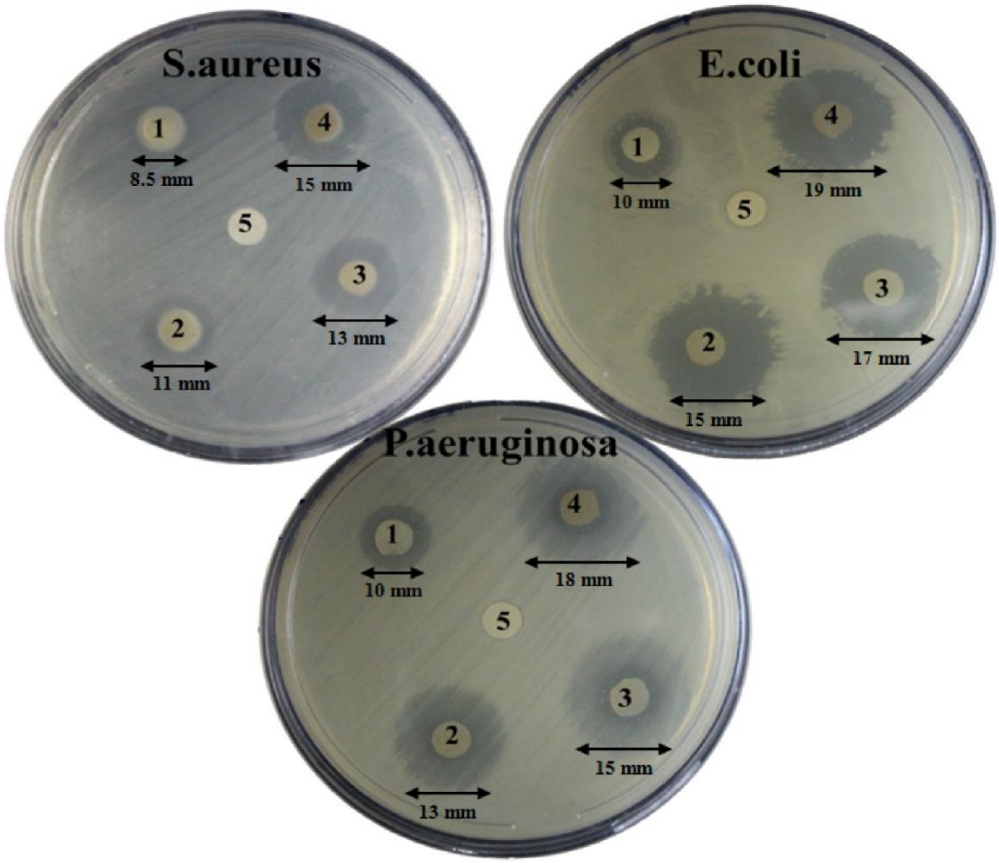

Figure 7- Antibacterial assessment of nanofiber scaffolds against *S. aureus*, *E. coli*, and *P. aeruginosa*; 1: CS/PEO nanofiber, 2: CS/PEO nanofiber containing 25% w/w extract, 3: CS/PEO nanofiber containing 25% w/w extract and 0.5% w/w GO, 4: CS/PEO nanofiber containing 25% w/w extract and 1% w/w GO, 5: negative control

4. Conclusion

A. lappa was extracted and used to fabricate electrospun CS/PEO/extract/GO nanofibers. An applied voltage of 20 kV, a flow rate of 0.4 ml/h, and a needle tip-to-rotor collector distance of 18 cm were identified as the optimum parameters to obtain more uniform CS/PEO nanofibers. In XRD analysis, the nanofibers containing 25% w/w extract showed peaks at 2θ = 18.97° and 22.19°, and addition of GO to CS/PEO/25% w/w extract resulted in slightly sharper peaks. The TGA curves indicated that CS/PEO/25% w/w extract/0.5% w/w GO nanocomposite had better thermal stability than other scaffolds. The initial decomposition temperature for CS/PEO/25% w/w extract and CS/PEO/25% w/w/0.5% w/w GO nanocomposites were about 246 and 264 °C, respectively. The antibacterial tests revealed that addition of 1% w/w GO to CS/PEO/25% w/w extract nanofiber exhibited better performance against Gram-negative bacteria than Gram-positive bacteria. According to FE-SEM images, thermal stability, and antibacterial properties, CS/PEO/25% w/w extract containing 0.5 and 1% w/w GO were recognized as the appropriate composition to fabricate electrospun nanofibers with uniform and defect-free morphologies. In general, these scaffolds indicated their potential for applications in bioengineering and wound care purposes. However, further studies are recommended to explore their long-term biocompatibility and safety.

5. Acknowledgment

The authors are grateful to the Guilan Science and Technology Park, and Halal Research Center of IRI., Iran Food and Drug Administration, Ministry of Health and Medical Education, Tehran, Iran.

6. Conflict of interest

The authors declare that there is no conflict of interest.

References

1. Yadav N, Parveen S, Chakravarty S, Banerjee M. Skin anatomy and morphology. Skin Aging & Cancer: Ambient UV-R Exposure. 2019: 1-10. https://doi.org/10.1007/978-981-13-2541-0_1

2. Gilaberte Y, Prieto-Torres L, Pastushenko I, Juarranz Á. Anatomy and Function of the Skin, in Nanoscience in dermatology. Elsevier. 2016: 1-14. https://doi.org/10.1016/B978-0-12-802926-8.00001-X

3. Irfan-Maqsood M. Classification of wounds: know before research and clinical practice. Journal of Genes and Cells. 2018; 4(1): 1-4. https://doi.org/10.15562/gnc.61

4. Rodrigues M, Kosaric N, Bonham CA, Gurtner GC. Wound healing: a cellular perspective. Physiological Reviews. 2019; 99(1): 665-706. https://doi.org/10.1152/physrev.00067.2017

5. Tottoli EM, Dorati R, Genta I, Chiesa E, Pisani S, Conti B. Skin wound healing process and new emerging technologies for skin wound care and regeneration. Pharmaceutics. 2020; 12(8): 735. https://doi.org/10.3390/pharmaceutics12080735

6. Versteeg HH, Heemskerk JW, Levi M, Reitsma PH. New fundamentals in hemostasis. Physiological Reviews. 2013; 93(1): 327-358. https://doi.org/10.1152/physrev.00016.2011

7. Jaffary F, Nilforoushzadeh MA, Sharifian H, Mollabashi Z. Wound healing in animal models. Tehran University of Medical Sciences Journal. 2017; 75(7): 471-479.

8. Dong R, Guo B. Smart wound dressings for wound healing. Nano Today. 2021; 41: 101290. https://doi.org/10.1016/j.nantod.2021.101290

9. Chen K, Hu H, Zeng Y, Pan H, Wang S, Zhang Y, et al. Recent advances in electrospun nanofibers for wound dressing. European Polymer Journal. 2022; 178: 111490. https://doi.org/10.1016/j.eurpolymj.2022.111490

10. Supaphol P, Suwantong O, Sangsanoh P, Srinivasan S, Jayakumar R, Nair SV. Electrospinning of biocompatible polymers and their potentials in biomedical applications. Biomedical Applications of Polymeric Nanofibers. 2012: 213-239. https://doi.org/10.1007/12_2011_143

11. Partovi A, Khedrinia M, Arjmand S, Ranaei Siadat SO. Electrospun nanofibrous wound dressings with enhanced efficiency through carbon quantum dots and citrate incorporation. Scientific Reports. 2024; 14(1): 19256. https://doi.org/10.1038/s41598-024-70295-9

12. Ahmed A, Xu L, Yin J, Wang M, Khan F, Ali M. High-throughput fabrication of chitosan/poly (ethylene oxide) nanofibers by modified free surface electrospinning. Fibers and Polymers. 2020; 21: 1945-1955. https://doi.org/10.1007/s12221-020-1109-9

13. Aranaz I, Alcántara AR, Civera MC, Arias C, Elorza B, Heras Caballero A, et al. Chitosan: an overview of its properties and applications. Polymers. 2021; 13(19): 3256. https://doi.org/10.3390/polym13193256

14. Raafat D, Sahl HG. Chitosan and its antimicrobial potential–a critical literature survey. Microbial Biotechnology. 2009; 2(2): 186-201. https://doi.org/10.1111/j.1751-7915.2008.00080.x

15. Lin SH, Ou SL, Hsu HM, Wu JY. Preparation and characteristics of polyethylene oxide/curdlan nanofiber films by electrospinning for biomedical applications. Materials. 2023; 16(10): 3863. https://doi.org/10.3390/ma16103863

16. Wang D, Cheng W, Wang Q, Zang J, Zhang Y, Han G. Preparation of electrospun chitosan/poly (ethylene oxide) composite nanofibers reinforced with cellulose nanocrystals: structure, morphology, and mechanical behavior. Composites Science and Technology. 2019; 182: 107774. https://doi.org/10.1016/j.compscitech.2019.107774

17. Mir SA, Dar LA, Ali T, Kareem O, Rashid R, Khan NA, et al. *Arctium lappa*: a review on its phytochemistry and pharmacology. In: Masoodi MH, Rehman MU (eds.). Edible Plants in Health and Diseases, Volume II: Phytochemical and Pharmacological Properties. 2022: 327-348. https://doi.org/10.1007/978-981-16-4959-2_10

18. Chan YS, Cheng LN, Wu JH, Chan E, Kwan YW, Lee SMY, et al. A review of the pharmacological effects of *Arctium lappa* (burdock). Inflammopharmacology. 2011; 19(5): 245-254. https://doi.org/10.1007/s10787-010-0062-4

19. Wang D, Bădărau AS, Swamy MK, Shaw S, Maggi F, Da Silva LE, et al. Arctium species secondary metabolites chemodiversity and bioactivities. Frontiers in Plant Science. 2019; 10: 834. https://doi.org/10.3389/fpls.2019.00834

20. Sun Q, Liu K, Shen X, Jin W, Jiang L, Saeed Sheikh M, et al. A novel anticancer agent isolated from plant *Arctium Lappa* L. Molecular Cancer Therapeutics. 2014; 13(1): 49-59. https://doi.org/10.1158/1535-7163.MCT-13-0552

21. Jiříčková A, Jankovský O, Sofer Z, Sedmidubský D. Synthesis and applications of graphene oxide. Materials. 2022; 15(3): 920. https://doi.org/10.3390/ma15030920

22. Ghulam AN, Dos Santos OA, Hazeem L, Pizzorno Backx B, Bououdina M, Bellucci S. Graphene oxide (GO) materials- Applications and toxicity on living organisms and environment. Journal of Functional Biomaterials. 2022; 13(2): 77. https://doi.org/10.3390/jfb13020077

23. Mathews A, Arbal AV, Kaarunya A, Jha PK, Le-Bail A, Rawson A. Conventional vs modern extraction techniques in the food industry. In: Jafari SM, Akhavan-Mahdavi S (eds.). Extraction processes in the food industry. Elsevier. 2024: 97-146. https://doi.org/10.1016/B978-0-12-819516-1.00013-2

24. Senapati MR, Behera PC. Novel extraction conditions for phytochemicals. In: Pati S, Sarkar T, Lahiri D (eds.). Recent frontiers of phytochemicals. Elsevier. 2023: 27-61. https://doi.org/10.1016/B978-0-443-19143-5.00019-0

25. Yuan TT, Jenkins PM, DiGeorge Foushee AM, Jockheck-Clark AR, Stahl JM. Electrospun chitosan/polyethylene oxide nanofibrous scaffolds with potential antibacterial wound dressing applications. Journal of Nanomaterials. 2016; 2016(1): 6231040. https://doi.org/10.1155/2016/6231040

26. Singh YP, Dasgupta S, Nayar S, Bhaskar R. Optimization of electrospinning process & parameters for producing defect-free chitosan/polyethylene oxide nanofibers for bone tissue engineering. Journal of Biomaterials Science, Polymer Edition. 2020; 31(6): 781-803. https://doi.org/10.1080/09205063.2020.1718824

27. Nezarati RM, Eifert MB, Cosgriff-Hernandez E. Effects of humidity and solution viscosity on electrospun fiber morphology. Tissue Engineering Part C: Methods. 2013; 19(10): 810-819. https://doi.org/10.1089/ten.tec.2012.0671

28. Mpukuta O, Dincer K, Özaytekin İ. Effect of dynamic viscosity on nanofiber diameters and electrical conductivity of polyacrylonitrile nanofibers doped nano-cu particles. International Journal of Innovative Engineering Applications. 2020; 4(1): 1-8. https://doi.org/10.46460/ijiea.707142

29. Najafiasl M, Osfouri S, Azin R, Zaeri S. The effect of adding alginate natural polymer on the structure of polyvinyl alcohol biocompatible nanofibers in electrospinning process. Iranian South Medical Journal. 2019; 22(1): 29-40.

30. Mahdizadeh S, Mokhtari-Hosseini ZB, Hatamian-Zarmi A, Ebrahimi-Hosseinzadeh B. Optimization of PVA/nano-bentonite nanofiber composite production for improving mechanical and thermal properties. Journal of Applied Research of Chemical-Polymer Engineering. 2018; 2(2): 17-28.

31. de Souza EJD, dos Santos FN, Pires JB, Kringel DH, da Silva WMF, Meinhart AD, et al. Production and optimization of ultrafine fiber from yam starch by electrospinning method using multivariate analysis. Starch. 2021; 73(3-4): 2000174. https://doi.org/10.1002/star.202000174

32. Azar R, Moslehi Aragh M, Rezaei AH. Investigation of morphology and production efficiency of produced nano-fibers with multi-nozzle electrospinning process. Journal of New Materials. 2018; 9(33): 97-112.

33. Mahdizadeh B, Maleknia L, Amirabadi A, Shabani M. Preparation of bio-sensor with nanofibers of glucose oxidase/chitosan/graphene oxide for detection of glucose. Iranian Journal of Chemistry and Chemical Engineering. 2022; 41(12): 4000-4014. https://doi.org/10.30492/ijcce.2022.538212.4917

34. Leng XX, Chiang SW, Du HD, Kang FY. Preparation and properties of electrospun GO/PEO nanofibers. New Carbon Material. 2018; 33(2): 125-130.

35. Zgura I, Badea N, Enculescu M, Maraloiu VA, Ungureanu C, Barbinta-Patrascu ME. Burdock-derived composites based on biogenic gold, silver chloride and zinc oxide particles as green multifunctional platforms for biomedical applications and environmental protection. Materials. 2023; 16(3): 1153. https://doi.org/10.3390/ma16031153

36. Hakimi F, Jafari H, Hashemikia S, Shabani S, Ramazani A. Chitosan-polyethylene oxide/clay-alginate nanofiber hydrogel scaffold for bone tissue engineering: preparation, physical characterization, and biomimetic mineralization. International Journal of Biological Macromolecules. 2023; 233: 123453. https://doi.org/10.1016/j.ijbiomac.2023.123453

37. Dey A, Karan S, De S. Effect of nanofillers on thermal and transport properties of potassium iodide–polyethylene oxide solid polymer electrolyte. Solid State Communications. 2009; 149(31-32): 1282-1287. https://doi.org/10.1016/j.ssc.2009.05.021

38. Hegazy DE, Mahmoud GA. Radiation synthesis and characterization of polyethylene oxide/chitosan-silver nanocomposite for biomedical applications. Arab Journal of Nuclear Sciences and Application. 2014; 47: 1-14.

39. Hashemikia S, Farhangpazhouh F, Parsa M, Hasan M, Hassanzadeh A, Hamidi M. Fabrication of ciprofloxacin-loaded chitosan/polyethylene oxide/silica

nanofibers for wound dressing application: in vitro and in vivo evaluations. International Journal of Pharmaceutics. 2021; 597: 120313. https://doi.org/10.1016/j.ijpharm.2021.120313

40. Saadat S, Emam-Djomeh Z, Askari G. Antibacterial and antioxidant gelatin nanofiber scaffold containing ethanol extract of pomegranate peel: Design, characterization and in vitro assay. Food and Bioprocess Technology. 2021; 14: 935-944. https://doi.org/10.1007/s11947-021-02616-z

41. Shyam M, Sabina EP. Harnessing the power of *Arctium lappa* root: a review of its pharmacological properties and therapeutic applications. Natural Products and Bioprospecting. 2024; 14(1): 49. https://doi.org/10.1007/s13659-024-00466-8

42. Acurio E, García-Cruz L, Montiel V, Iniesta J. Preparation of poly(vinyl) alcohol/chitosan hybrid membranes doped with graphene nanosheets. Advanced Materials & Technologies. 2017; 1: 9-19. https://doi.org/10.17277/amt.2017.01.pp.009-019